Chemical Looping Technology: Oxygen Carrier Characteristics

Siwei Luo, Liang Zeng, and Liang-Shih Fan*

William G. Lowrie Department of Chemical and Biomolecular Engineering, The Ohio State University, Columbus, Ohio 43210; email: luo.92@osu.edu, zeng.40@osu.edu, fan.1@osu.edu

Annu. Rev. Chem. Biomol. Eng. 2015. 6:53–75

First published online as a Review in Advance on April 16, 2016

The *Annual Review of Chemical and Biomolecular Engineering* is online at chembioeng.annualreviews.org

This article's doi: 10.1146/annurev-chembioeng-060713-040334

Keywords

energy, syngas, combustion, partial oxidation, metal oxides

Abstract

Chemical looping processes are characterized as promising carbonaceous fuel conversion technologies with the advantages of manageable CO_2 capture and high energy conversion efficiency. Depending on the chemical looping reaction products generated, chemical looping technologies generally can be grouped into two types: chemical looping full oxidation (CLFO) and chemical looping partial oxidation (CLPO). In CLFO, carbonaceous fuels are fully oxidized to CO_2 and H_2O, as typically represented by chemical looping combustion with electricity as the primary product. In CLPO, however, carbonaceous fuels are partially oxidized, as typically represented by chemical looping gasification with syngas or hydrogen as the primary product. Both CLFO and CLPO share similar operational features; however, the optimum process configurations and the specific oxygen carriers used between them can vary significantly. Progress in both CLFO and CLPO is reviewed and analyzed with specific focus on oxygen carrier developments that characterize these technologies.

INTRODUCTION

Carbonaceous fuels, including both fossil fuels and biomass, are estimated to supply more than 80% of the global energy consumption through 2040 (1). Their utilization can be generally grouped into two reaction types: full oxidation and partial oxidation. Full oxidation, namely, combustion, binds oxygen with carbon and hydrogen atoms, forming CO_2 and H_2O, respectively. Maximum thermal energy can be released through the full oxidation process for heat and power generation. In contrast, partial oxidation binds a part of the carbon and/or hydrogen atoms with oxygen, minimizing the formation of CO_2 and H_2O. The partial oxidation products include synthesis gas (syngas, a mixture of primarily CO and H_2) and hydrocarbons with less oxygen content, such as olefins and aromatic hydrocarbons, which are important intermediates for liquid fuel and chemical synthesis. The current processes for both full and partial oxidation, however, are not sufficiently efficient. Furthermore, the quantity and quality of carbonaceous fuels are rapidly declining. To sustain these feedstocks, alternative fuel conversion technologies with low environmental impacts and high energetic efficiencies are highly desired. The chemical looping technology promises to be a transformational way for clean and efficient fuel conversion to electricity, hydrogen, and syngas, as shown in **Figure 1**.

Conventional combustion approaches directly mix carbonaceous fuel feed with air, generating a CO_2-containing flue gas that is emitted to the atmosphere. Current concerns over climate change bear relevance to CO_2 emission (2). The development of cost-effective CO_2 capture techniques for fossil fuel combustion processes thus becomes important. The US Department of Energy recognizes chemical looping combustion (CLC) or chemical looping full oxidation (CLFO) as one of the most advanced electric power generation techniques in a carbon-constrained scenario (3). **Figure 2** shows a simplified process flow diagram of a coal-fired CLC system. When

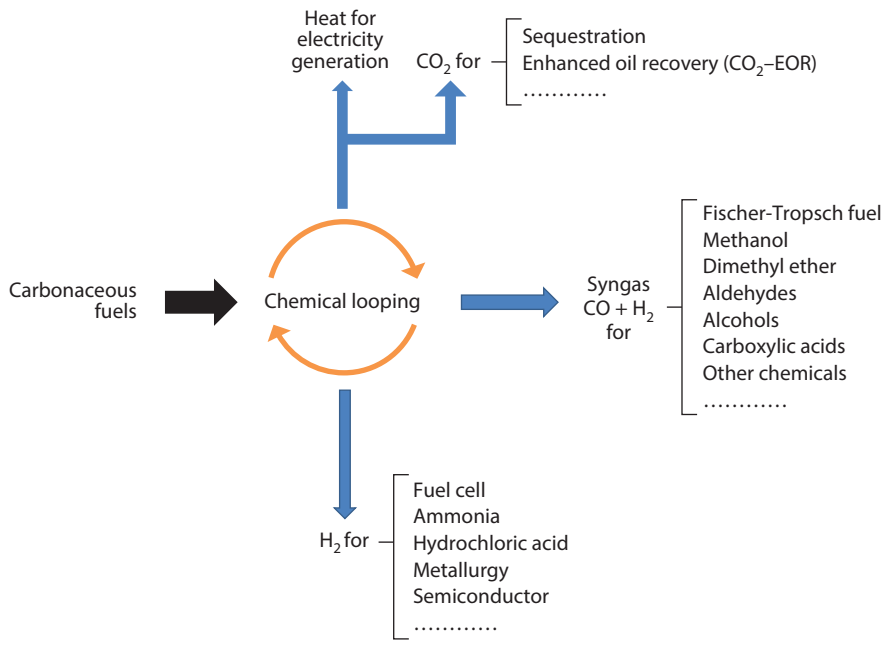

Figure 1

Chemical looping processes for carbonaceous fuels conversion.

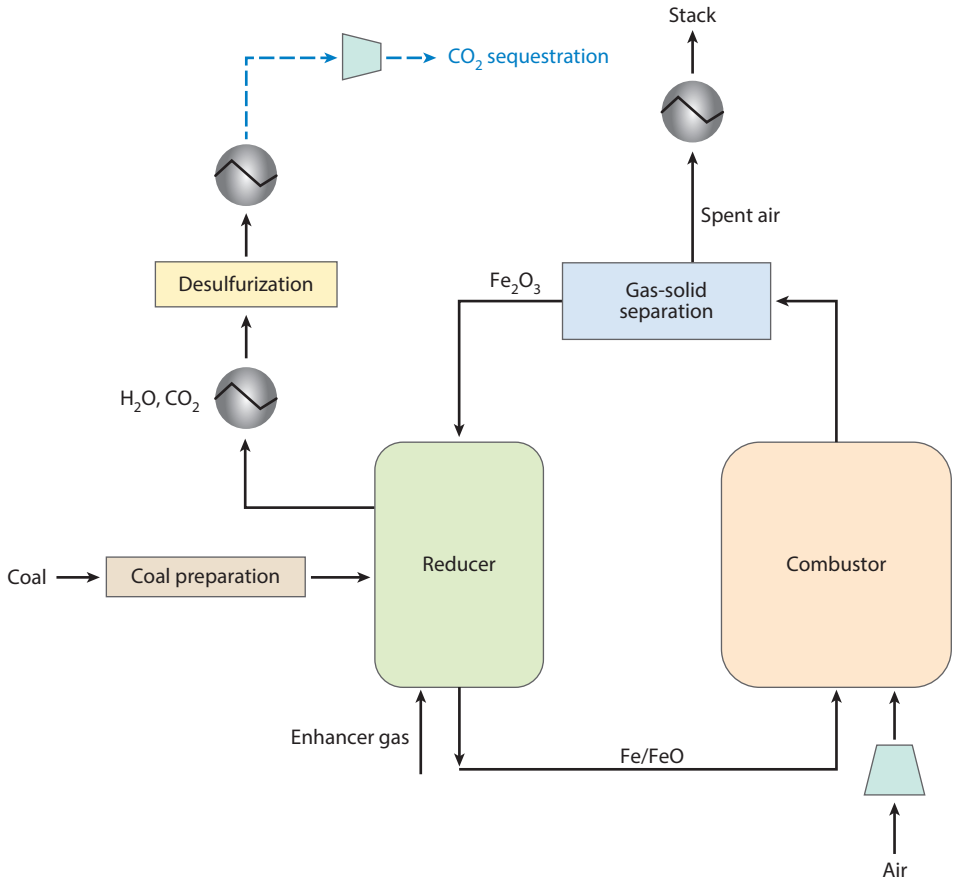

Figure 2

Simplified process flow diagram of a chemical looping combustion system.

considering the exergy of CLC and conventional combustion systems, CLC yields greater energy conversion efficiency owing to the reduced irreversibility of the combustion reactions (4, 5). The reaction path design prevents the direct contact of air with the fuel source, resulting in the production of a concentrated CO_2 flue gas without the need to employ energy-intensive gas-gas separation schemes. The CLC processes are capable of achieving more than 90% CO_2 capture with less than 30% increment in the cost of electricity (6).

Partial oxidation of carbonaceous fuels provides a viable way to produce syngas, olefins, and other chemicals. Among these products, syngas and hydrogen are considered core chemical intermediates to produce other valuable products. Currently, steam methane reforming (SMR) is the dominant industrial approach for syngas and hydrogen production. This conventional approach requires a significant amount of steam (H_2O/CH_4 molar ratio of 1 to 3) to enhance the conversion of CH_4 (7, 8). The excess steam promotes the water-gas shift reaction, resulting in a hydrogen-rich syngas stream that is good for hydrogen production but is not desirable for methanol production or Fischer–Tropsch synthesis. Furthermore, the energy penalty associated with steam generation and condensation drastically decreases the thermal efficiency of SMR. Partial oxidation of methane and autothermal reforming technologies have been commercialized for gas-to-liquid processes. However, these technologies are costly, as they require high-purity oxygen from capital-intensive

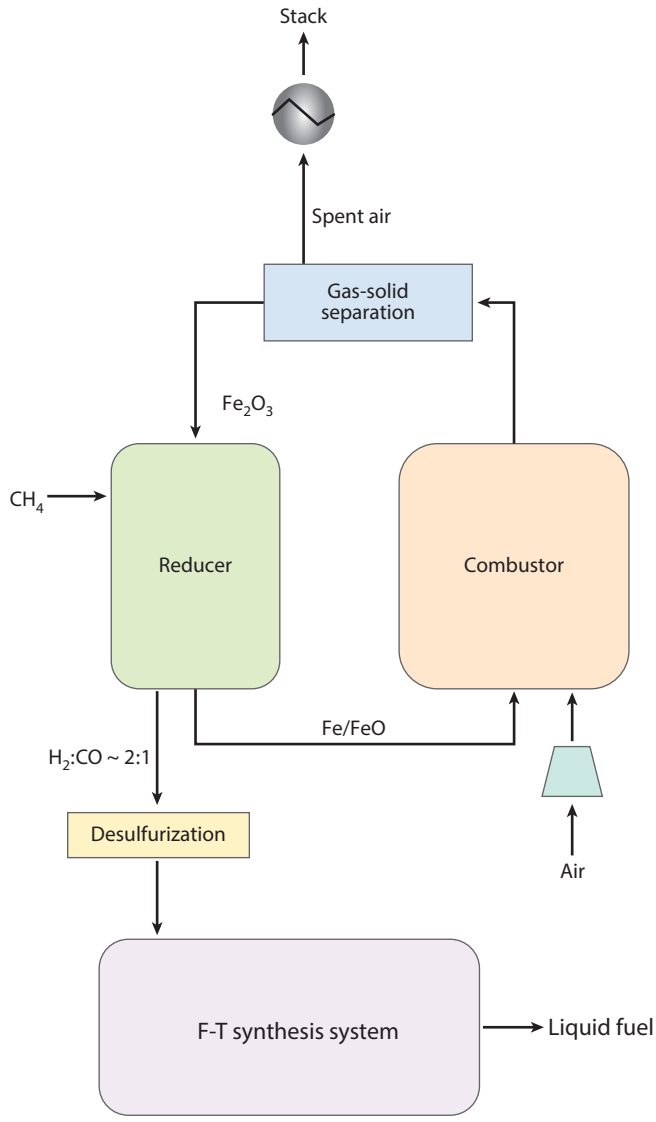

Figure 3

Simplified process flow diagram of a chemical looping gasification system for liquid fuel synthesis.

air separation units. Alternatively, in recent years, chemical looping partial oxidation (CLPO) has emerged as an attractive approach to producing syngas and hydrogen from various fuel feedstocks, such as natural gas and coal, including chemical looping gasification (CLG) and chemical looping reforming (CLR) (5, 9–11). **Figure 3** shows a simplified natural gas–fueled CLG system for liquid-fuel synthesis. CLPO requires minimal or no external steam as compared with the steam requirements of SMR and has a potential to produce high-quality syngas with high CO and H_2 concentrations and desirable CO/H_2 ratios.

As shown in **Figure 4**, CLFO and CLPO share similar characteristics in using metal oxides (in most cases) as oxygen carriers to transfer oxygen from the air source to the fuel source. Both

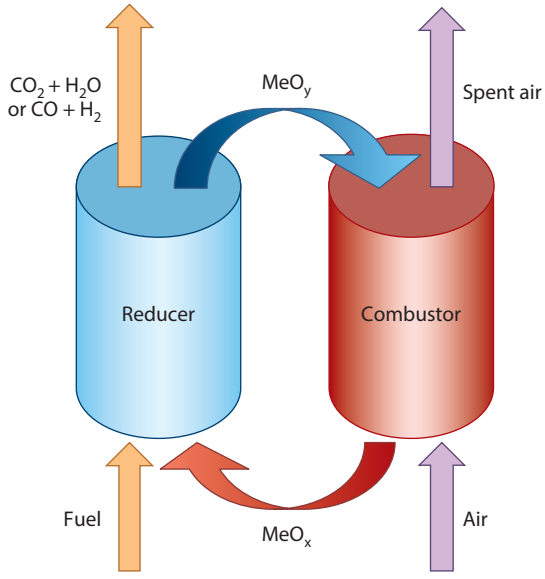

Figure 4

General schemes of chemical looping full and partial oxidation (x > y).

chemical looping systems consist of a reducer (or fuel) reactor and an oxidizer (or air) reactor. Chemical looping processes use solid oxygen carrier materials, such as metal oxides or sulfates, to indirectly provide oxygen for full or partial oxidation of the fuel in the reducer. The oxygen-depleted oxygen carriers are then regenerated by a reaction with air in the oxidizer while releasing heat for process duty and/or power generation. Although solid oxygen carriers are circulated between two reactors for heat and oxygen transfer, the resulting gases are segregated, yielding a high-purity CO_2/syngas stream from the reducer and an O_2-depleted flue gas from the oxidizer. By this redox reaction scheme, minimal energy is consumed for high-purity CO_2 separation or syngas production.

Oxygen carrier materials play a key role in determining the chemical looping product quality and process efficiency. Extensive research has been conducted to develop desirable oxygen carrier materials. To optimize the process, it is necessary to consider the key oxygen carrier materials characteristics: redox reactivity, long-term stability, physical strength, toxicity, and production cost. Thousands of oxygen carrier materials have been studied for CLFO/CLPO applications (12, 13). During the early development of these applications, single metal oxides or sulfates were considered as the active components in the oxygen carrier materials. Recent research has been guided toward the use of multiple metal-based composite materials for improved process performance. The development of oxygen carrier materials for CLFO and CLPO is reviewed and discussed in the following sections.

OXYGEN CARRIERS FOR CHEMICAL LOOPING FULL OXIDATION

Single Metal–Based Materials

In the reduction step for CLFO processes, the oxygen carrier must provide adequate oxidation capacity to fully convert carbonaceous fuels to CO_2 and H_2O. Incomplete fuel conversion will result in additional posttreatment steps, decreasing the overall process efficiency and increasing

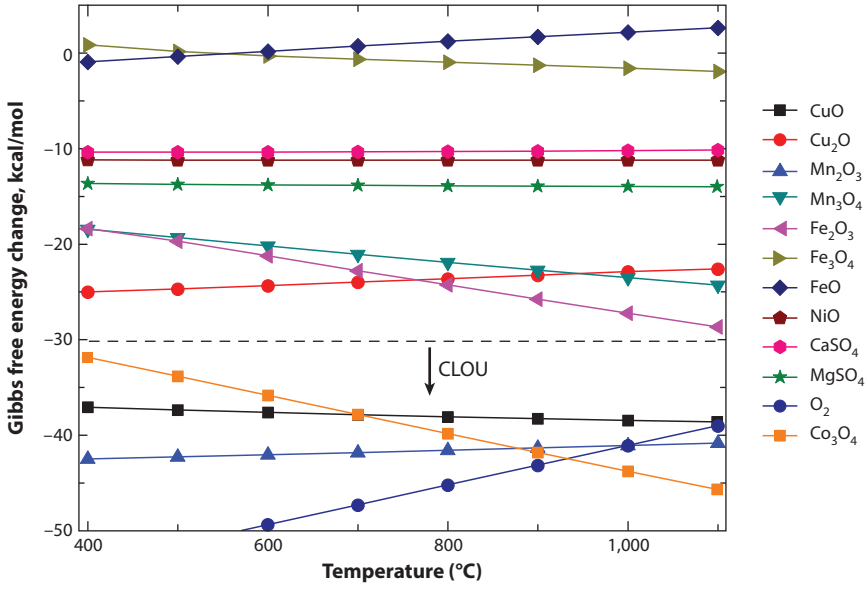

Figure 5

Gibbs free energy change of oxygen carrier reduction with 1 mol of CO.

the operating costs. The reduction extent of the oxygen carrier also affects the overall solids circulation rate, which has a significant effect on the chemical looping process efficiency. In the oxidation step, the oxygen carrier needs to be regenerated with minimal excess air usage to reduce the associated air compression cost. The redox behavior of the oxygen carrier largely depends on the thermochemical properties of its primary metal oxide.

Figure 5 illustrates the Gibbs free energy (ΔG) variation with temperature for CO and oxygen carrier reactions calculated from HSC Chemistry. This figure is presented based on 1 mol of CO reacting with the metal oxides/sulfates at 1 atm. **Figure 5** provides information that can be used to evaluate the reduction and oxidation potentials of oxygen carrier materials. The positions of the lines in **Figure 5** indicate relative reducing and oxidizing capabilities of different materials. During the oxygen carrier reduction step, to fully convert fuels to CO_2 and H_2O, the metal oxide/sulfate lines must be located at lower positions in **Figure 5**. Based on this consideration, materials such as Cu-, Mn-, Co-, Fe-, and Ni-based transition metal oxides and Ca-based alkaline earth sulfates can be used for CLC applications.

Chemical looping with oxygen uncoupling metal oxides. Among the above-mentioned candidates in **Figure 5**, the CuO, Co_3O_4, and Mn_2O_3 lines approach the O_2 line at temperatures above 800°C, indicating that under high temperatures, these oxides can release O_2 to the gas phase. The chemical looping process using these metal oxides for gaseous oxygen release is referred to as chemical looping with oxygen uncoupling (CLOU) (14). CLOU is advantageous for fuel combustion applications because the reducer reactions are net exothermic and the CLOU materials have higher reaction rates as compared with the reaction rates of metal oxides/sulfates that use lattice oxygen for fuel reactions. The exothermic reaction eases the heat integration for the entire process system, whereas the faster kinetics reduces the reducer size. **Figure 5** shows that, at high temperatures, Co_3O_4 and Mn_2O_3 lines are below the line that corresponds to pure O_2 reaction with CO. Thus, it is difficult to regenerate Co_3O_4 and Mn_2O_3 using ambient air. The

low–oxygen carrying capacities of cobalt and manganese oxides also prohibit their effective use as oxygen carriers.

Copper oxides are considered promising materials for CLOU processes. The use of CuO for chemical looping applications can be dated back to the mid-twentieth century (15). The theoretical oxygen carrier capacity by weight is 10% from CuO to Cu_2O and 20% from CuO to Cu. **Figure 5** shows that gaseous O_2 decomposition can occur only from CuO to Cu_2O, though Cu_2O still possesses a high oxidation capability for full CO conversion. Studies indicate that the Cu_2O regeneration to CuO is slower than the reduction of CuO to Cu_2O. From **Figure 5**, the CuO line is close to the O_2 line, indicating that the ambient air has a small thermodynamic driving force for Cu_2O oxidation. Additionally, the formation of the CuO layer during the regeneration step also reduces the diffusion process of O_2 that further slows down its reoxidation rate (16).

The ICB-CSIC (Institute of Carbochemistry/Instituto de Carboquímica, Consejo Superior de Investigaciones Científicas) group has extensively studied copper-based oxygen carriers using various support materials and synthesis methods (17–22). For example, CuO supported with Al_2O_3 oxygen carriers was synthesized using the impregnation method. The results showed that a full methane conversion could be achieved. However, a significant amount (>80% wt) of support materials coupled with carefully controlled operating temperature (<950°C) was needed to accommodate the low copper-melting point (18). Specifically, when the CuO content is greater than 20% by weight, particle agglomeration may occur, resulting in bed defluidization. A large amount of support was also needed to reduce the possibility of forming Cu_2S (20). The Chalmers University research group indicated that at temperatures over 1,000°C, CuO and Al_2O_3 would form a spinel structure of $CuAl_2O_4$, resulting in a loss of the unique CLOU property. The redox pair of $CuAl_2O_4$-$CuAlO_2$ is not stable, as $CuAlO_2$ has very slow oxidation kinetics and can become inactive after several cycles (23). However, when CuO is supported on $MgAl_2O_4$, this compound can avoid the interaction between the primary and support materials, allowing for the CLOU properties of CuO to be maintained (23). Using the freeze-granulation synthesis method, Lyngfelt et al. (24) achieved a satisfactory CLC performance using methane and woody biomass when ~40% CuO was supported by $MgAl_2O_4$. The CSIC group also identified that when using mechanical mixing and pelletizing methods, the CuO content can be up to 60% and 40% with $MgAl_2O_4$ and ZrO_2 support materials, respectively, without inducing particle agglomeration (22).

In other efforts, Xu et al. (25) used inexpensive cement support materials and mechanical mixing to prepare copper-based CLOU materials, which demonstrated good results. Song et al. (26) attempted the synthesis of Al_2O_3-supported CuO materials using layered double hydroxides as precursors. The formation of $NaAlO_2$ from residual sodium was noted to inhibit the formation of Cu-Al compounds. Such a synthesis method can promote nanostructure formation and improve the homogeneous dispersion of Cu cations, yielding better reactivity and stability for CLOU applications.

Non-CLOU metal oxides. Nickel and iron oxides have been widely studied for CLC and tested in many reactor configurations. As shown in **Figure 5**, they are located further away from the CLOU materials region, and their lattice oxygen can be transferred to fuels via gas intermediates, such as CO_2/CO and H_2O/H_2. NiO possesses good reaction kinetics with gaseous fuels. However, for a solid fuel conversion, this advantage becomes insignificant owing to the slow solid fuel gasification reaction. Additionally, from **Figure 5**, the maximum CO conversion is 99.5% owing to the close proximity of the NiO reduction line to the $\Delta G = 0$ line. The high materials cost and the health effects also deter the commercial use of nickel-based oxygen carriers in chemical looping processes.

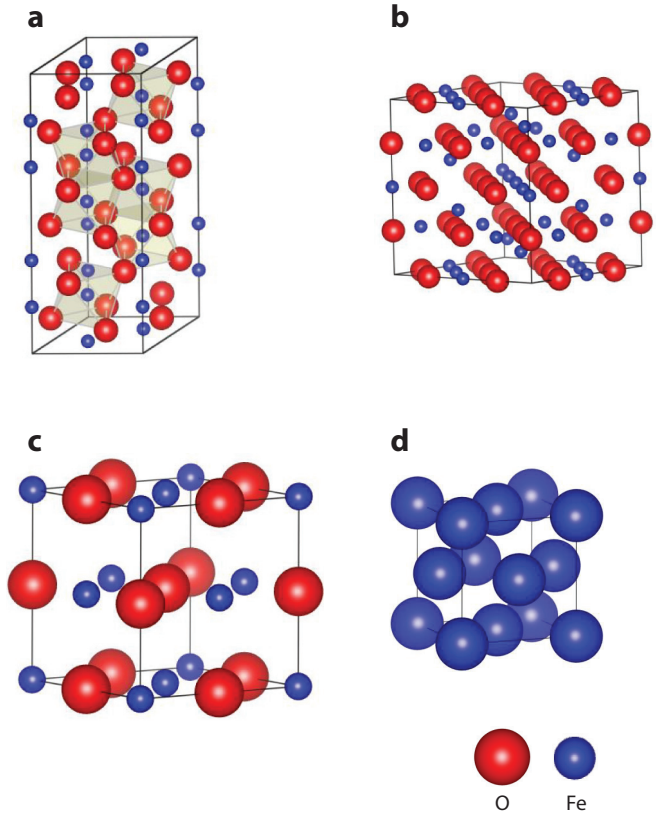

Figure 6

Structures of (*a*) Fe_2O_3, (*b*) Fe_3O_4, (*c*) FeO, and (*d*) γ-Fe.

Iron oxides are cheap and nontoxic, with high melting points and high mechanical strengths. From **Figure 5**, Fe_2O_3 has a greater oxidizing capability than NiO, thus allowing iron oxides to fully convert the carbonaceous fuel to CO_2 and H_2O.

Iron oxide reactions with fuels are a complex process owing to their stepwise reduction from Fe_2O_3 to Fe_3O_4, to FeO, and to Fe. Fan et al. (27–33) reported about the characteristics of multiple oxidation states of iron and developed a countercurrent moving bed reactor system for their application in chemical looping systems. The structures of iron oxides are shown in **Figure 6**. Each oxidation state corresponds to a different crystal structure that includes rhombohedral (α-Fe_2O_3), inverse spinel (Fe_3O_4), rock salt cubic (FeO), and body-centered cubic (Fe) structures. On one hand, Fe_2O_3, Fe_3O_4, and FeO possess similar close-packed oxygen structures, which render the redox transitions between each phase faster than that between the lower oxidation phases of FeO and Fe (34, 35). On the other hand, even though there exists a minor variation from the hexagonal close-packed structure to the cubic close-packed structure, Fe_2O_3 reduction to Fe_3O_4 could lead to an irreversible structure change, such as volume expansion, as the reaction proceeds (36). Coupled with the sintering effects at high operating temperatures, pure iron oxides can quickly lose reactivity and oxygen-carrying capacity after the first several redox cycles. When suitable support materials are added, the reactivity and recyclability of iron-based oxygen carriers can be drastically improved. For example, Xiang et al. (37) studied iron oxide materials mechanically mixed with Al_2O_3 and TiO_2 as supports. They showed that both supports provided stable reactivity and mechanical

strength over three to ten redox cycles. They concluded that oxygen carriers with 60% Fe_2O_3 and 40% Al_2O_3 presented the best performance. The postexperimental results indicated that there was no formation of inactive $FeAl_2O_4$. They attributed the oxygen carriers' high reactivity to the high porosity and surface area, which could increase the gaseous intraparticle diffusion and surface reaction rate.

Phase separation is another cause for oxygen carrier materials degradation, as the iron phase may segregate and sinter. To prevent this behavior, Liu & Zachariah (38) doped potassium to Al_2O_3-supported iron oxides and showed improved reactivity, stability, CO_2 product selectivity, and carbon deposition resistance. The K ions could assist in binding Fe and Al, thereby reducing the potential for phase separation.

Li et al. (39) investigated TiO_2-supported iron oxide oxygen carriers using an inert marker experiment in combination with density functional theory (DFT) calculations. The results indicate that pure iron oxide oxidation is dominated by Fe cation outward diffusion, whereas the TiO_2-supported iron oxide is dominated by O anion inward diffusion. These results are due to the different structures between Fe_2O_3 and TiO_2, which create a considerable amount of oxygen vacancies enhancing oxygen ion diffusivity. This phenomenon explains why the reactivity of TiO_2-supported Fe_2O_3 can be maintained over multiple redox cycles while the pore volume and surface area significantly decrease during this cyclic process.

Metal sulfates. Several chemical looping studies have been performed using $CaSO_4$ as an oxygen carrier owing to its low cost and large oxygen carrying capacity. In **Figure 5**, the $CaSO_4$ line is above the NiO line. Therefore, the CO conversion is lower than 99.5%. **Figure 5** also shows that $MgSO_4$ has a higher oxidation capability than $CaSO_4$. Limited research has been conducted for $MgSO_4$. A challenge to metal sulfate CLC processes is the potential sulfur release to the product gas stream. Song et al. (40) studied the sulfur release mechanism for $CaSO_4$ and observed H_2S and SO_2 formation from the reducer and the oxidizer, respectively. At ~900°C, part of the sulfur in $CaSO_4$ will be lost during the $CaSO_4$-CaS cycle, and CaO will be accumulated in the system. To reduce the sulfur release, Song et al. (41) synthesized an oxygen carrier with 7% Fe_2O_3 and 93% $CaSO_4$, and the results showed that this modified material increased the fuel conversion to CO_2 while reducing the H_2S formation in the reactions.

As discussed above, individual metal oxide or sulfate materials have been widely studied for CLC applications, and yet, no desired single metal–based oxygen carrier has been identified for practical use. To further improve the oxygen carrier performance, the use of multiple metal–based materials was considered. For example, He et al. (42) proposed the use of bimetallic oxygen carrier particles with two active phases, CuO and Fe_2O_3. A small amount (5%) of additional CuO could significantly boost the solid fuel conversion by using its CLOU properties, whereas Fe_2O_3 could be maintained as the main active phase to avoid CuO sintering and to facilitate hydrogen generation. Inert support materials can be used to separate the two active metal oxides so they can behave actively individually. Other approaches include forming composite materials from multiple metal oxides, which is further discussed in the following section.

Multiple Metal–Based Materials

CLOU materials. Chalmers University conducted studies on multiple metal oxides to modify the thermodynamic property of manganese-containing materials for CLOU applications. Binary metal oxides tested included Mn-Fe, Mn-Ni, Mn-Si, Mn-Mg, and Mn-Cu; among them, Mn-Fe compounds demonstrated desired CLOU properties (43–46). In these studies, the properties of the Mn-Fe compound vary with the Mn content and operating temperatures. For example,

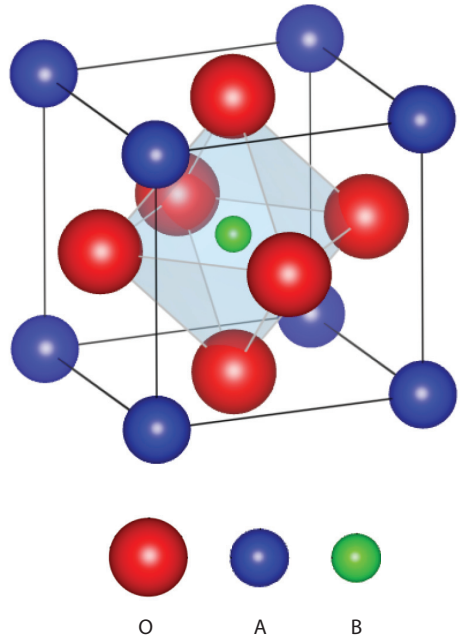

Figure 7

Structures of perovskite A(II)B(IV)O_3.

$(Mn_{0.8}Fe_{0.2})_2O_3$ bixbyite and $(Mn_{0.8}Fe_{0.2})_3O_4$ spinel are a good redox pair at 850°C, with excellent performance on methane and woody char (44). Further studies showed that low–Mn content (20–40%) materials can release oxygen at temperatures above 900°C, whereas high–Mn content (>50%) materials behave better at temperatures between 850°C and 900°C (45). Multiple redox tests were also conducted that showed an increased reactivity over the cycles owing to volume expansion and increased porosity (44). However, the volume expansion had a negative effect on mechanical strength and particle integrity.

Ternary metal oxides are also studied, with a focus on the variants of $CaMnO_{3-\delta}$ perovskites. Perovskite is a class of compounds with formulae of A(II)B(IV)O_3 that are known for their high oxygen conductivity, thermal stability, and other favorable properties (47–50). The structure of perovskite is shown in **Figure 7**. Perovskite structures are selected in light of their oxygen non-stoichiometry and fast oxygen-diffusion features. Furthermore, partial substitutions of atoms in B sites were found to result in improved catalytic effects owing to the lattice defects (51). Researchers developed complex oxygen carriers, such as $La_{1-x}Sr_xM_yFe_{1-y}O_3$ (M = Ni, Co, Cr, Cu), to achieve better reactivity. $CaMnO_{3-\delta}$ was found to be capable of releasing oxygen at high temperatures (52). Additionally, $CaMnO_{3-\delta}$ has a high mechanical strength, high melting point, and low cost, as it can be synthesized from calcium and manganese oxides. However, $CaMnO_{3-\delta}$ is not stable and can be easily decomposed to $CaMn_2O_4$ and $Ca_2MnO_{4-\delta}$. To maintain a stable perovskite structure during the redox process and to further improve the performance, several metal dopings have been considered, including Fe, Ti, Mg, Cu, and La (53–56). Among them, Mg could not substitute for the Mn site owing to its difference in ion size, and Cu-doped materials did not perform well owing to their defluidization behavior. $CaMn_{0.875}Ti_{0.125}O_{3-\delta}$ has shown high conversions with various fuels in a fluidized bed (53). However, the sulfur resistance of such compounds must

be further improved. The sulfur in the fuel can react with the Ti-doped perovskite structure to form $CaSO_4$ and accumulate during the redox cycles (56).

Non-CLOU materials. Several binary metal oxides have been examined based on their oxygen carrier performance. Iron-containing materials are considered as the key metal oxides owing to their low cost and reasonably good reactivity. Ferrites, usually MFe_2O_4-type spinels, are used for such materials. For example, redox cycles of $NiFe_2O_4$ and $CuFe_2O_4$ can be used for hydrogen production and storage via steam iron reaction, and these materials have also been studied for CLC applications (57). Kuo et al. (58) synthesized $NiFe_2O_4$ by ball milling and high-temperature calcination. The resulting materials showed better performance than single metal oxides such as Fe_2O_3 or NiO in terms of reactivity and recyclability. Wang et al. (59, 60) conducted both thermodynamic and kinetic studies on $CuFe_2O_4$. They concluded the binary oxygen carrier performed better with solid fuel than the single iron oxide–based materials. The reduced phases, depending on the temperature and fuel, were found to be Cu, Cu_2O, $CuFeO_2$, and/or Fe_3O_4. Such phase migration might lead to an irreversible structure change. Additionally, the formation of Cu_2S and Fe_2SO_4 was detected when reacting with high sulfur coke. These reactions affected the reactivity and recyclability. Weimer et al. (61) used atomic layer deposition to synthesize $Co_{0.85}Fe_{2.15}O_4$ and Fe_2O_3 composite thin films supported on ZrO_2, which showed good activities for hydrogen generation. A similar compound was presented for solar-based redox cycle for isothermal water-splitting reactions (62).

Naturally occurring minerals, such as ilmenite, have also been considered for CLC applications because of their low cost (63–66). For ilmenite, the redox cycles occur between Fe_2TiO_5 and $FeTiO_3$. Ilmenite exhibits a higher oxygen-carrying capacity compared with the redox cycle between Fe_2O_3 and Fe_3O_4. Li et al. (67) conducted ab initio simulations showing that the energy barrier for oxygen ion diffusivity in $FeTiO_3$ is also significantly lower than that in FeO, which suggested that faster kinetics could be obtained by using ilmenite. An activation and deactivation phase could be observed in the redox cycles using ilmenite, which could be attributed to the phase separation (65). The iron phase migrated to the surface during the oxidation of $FeTiO_3$, whereas the TiO_2 enlarged in the redox cycles, which could crack the ilmenite particle. The TiO_2 crystal formation is part of the Becher process and is widely used for titania production.

An optimal oxygen carrier should be determined based on its thermodynamic equilibrium, recyclability, synthesis method, resistance to attrition, and materials cost. The above discussion mainly focused on the oxygen carrier materials developed toward CLFO applications. Thursfield et al. (11) recently reviewed the materials used for hydrogen production using the chemical looping approach, whereas Li et al. (68) discussed possible oxygen carriers for syngas generation from natural gas. The following section discusses the oxygen carrier materials for CLPO applications, with a focus on syngas production.

OXYGEN CARRIERS FOR CHEMICAL LOOPING PARTIAL OXIDATION

Single Metal Oxide Materials

CeO_2. Ceria is a fluorite structure, which is considered to be favorable for rapid diffusion of oxygen. Otsuka et al. (69) investigated the partial oxidation of methane to syngas with cerium oxide in the 1990s. Their work defined the chemical looping scheme using lattice oxygen from ceria for partial oxidation of methane and subsequent regeneration of the materials. The reaction temperature for reduction of the oxygen carriers was greater than 700°C and ~500°C for regeneration. Thermodynamically, CH_4 oxidation with CeO_2 had a very high selectivity toward CO and

H_2 with full CH_4 conversion. However, this reaction was characterized by slow kinetics. Otsuka et al. (69) attempted to determine the rate-limiting step of the partial oxidation reaction. They believed that H_2 formation and desorption were slower steps than the CH_4 splitting reaction or lattice oxygen diffusion.

A significant amount of work has been conducted to enhance the ionic diffusivity of CeO_2-based materials. Various types of dopants have been incorporated into CeO_2 to increase its reactivity. For example, introduction of Sn ions was found to be able to increase reactivity. Gupta et al. (70) studied the effects of Sn ions using DFT calculations and found that Ce exhibits 4 + 4 coordination, whereas Sn exhibits 4 + 2 + 2 coordination. Because the metal-oxygen bond became weaker owing to the doping effect of Sn ions, the oxygen ion diffusivity was enhanced significantly. Furthermore, other types of metal oxides have also been discovered by researchers as promising dopants for ceria to increase oxygen conductivity; however, they have not been tested for chemical looping applications (71). Using γ-Al_2O_3-supported CeO_2 with Pt and Rh promoters could also increase the reaction rate as Pt accelerates the dissociation of the C-H bond (72). Mattos et al. (73) introduced ZrO_2 to the Pt-CeO_2 system and found that the reaction rate increased. It was suggested that $Ce_xZr_{1-x}O_2$ ($x > 0.5$) solution had a very high oxygen-storage capacity owing to its cubic fluorite structure, which enhanced the reactivity. The Ce-Zr-O solid solution was also a catalyst for the methane-reforming reaction (74). In some extreme cases, more ZrO_2, PrO_2, or TbO_2 was incorporated into the CeO_2 oxygen carriers. It was assumed that oxides of fluorite-type structure were critical for superior lattice oxygen reactivity and recyclability. Sadykov studied the effect of Sm and Bi dopants for the partial oxidation of methane with CeO_2 and found that the Ce-Sm-O solid solutions exhibited much higher reactivity and selectivity. However, Ce-Bi-O solid solutions exhibited decreasing selectivity toward syngas (75, 76). Although considerable research has been conducted along these lines with CeO_2 as the base material, carbon deposition on the catalyst still must be overcome (77–80).

NiO. NiO is one of the most extensively tested oxygen carriers for both CLC and reforming. The structure of NiO is similar to that of FeO. Because of its selectivity to CO_2 and H_2O, the NiO-to-fuel ratio must be controlled within a narrow range to generate the syngas with desirable concentrations and negligible carbon deposition. Because it is known that pure metal oxides lose their reactivity within a few cycles, most of the work with NiO as oxygen carriers for partial oxidation focuses on the selection of favorable support materials. Using the freeze granulation method, Johansson et al. (81) compared $MgAl_2O_4$ and $NiAl_2O_4$ as supports. They found that $MgAl_2O_4$ achieved a much higher methane conversion and had a lower tendency for carbon formation. Because the freeze granulation synthesis method was not economically viable for large-scale production, other oxygen carrier synthesis methods have been tested. Various preparation methods were also evaluated; it was found that deposition–precipitation methods produced oxygen carriers more resistant to carbon deposition than those prepared by dry impregnation (82). In addition, spray drying could be a promising alternative, as this method produced oxygen carriers with similar performance to that of oxygen carriers synthesized using freeze granulation (83). Zafar et al. (84) further tested NiO on SiO_2 and $MgAl_2O_4$ supports in a thermogravimetric analyzer. They found that SiO_2 reacted with primary metal oxides and formed stable unreactive silicates. The formation of silicates resulted in a poor recyclability with a high reactivity in the first few cycles. Lowering the reaction temperature alleviated the degradation but could not fully eliminate this characteristic. They concluded that $MgAl_2O_4$-supported NiO performed best for both full oxidation and partial oxidation (85). Additionally, different phases of Al_2O_3 support have also been tested. NiO with α-Al_2O_3 support demonstrated the highest reactivity; NiO with γ-Al_2O_3 had the lowest reactivity for the partial oxidation of methane. The low reactivity of Ni-γ-Al_2O_3

was attributed to the formation of $NiAl_2O_4$ (86). Additive materials have also been explored to increase the performance of the Ni-based oxygen carriers. For example, a small amount of $Ca(OH)_2$ dopant was found to increase the particle strength and, hence, its attrition resistance. MgO could also work as a promoter to increase the feedstock conversion at the early stage of the reaction (83). Furthermore, some demonstrations in a fluidized reactor have also been carried out for NiO-based oxygen carriers for partial fuel oxidation (86–89). This process is known as CLR of methane. However, owing to the materials cost and other reasons, NiO is not likely to be the material used for commercial CLPO use.

Fe_2O_3. Similar to NiO, Fe_2O_3 is another type of material that has been widely tested for chemical looping applications. Unlike NiO, the multiple oxidation states of Fe_2O_3 provide unique advantages for fuel partial oxidation when coupled with a favorable reactor design. Nakayama et al. (90) found that Fe_2O_3/Y_2O_3 with Rh_2O_3 as a promoter produced a high purity of syngas with 54% methane conversion. Steinfeld & Kuhn (91) proposed the coproduction of iron and syngas via partial oxidation of methane with Fe_3O_4 in a high-temperature reactor heated using solar thermal energy. This scheme could be altered to produce syngas and hydrogen if iron was regenerated with steam. Thermodynamically, Fe_3O_4 and CH_4 produce syngas with 67% H_2 and 33% CO at 1,027°C; however, the results did not show the equilibrium composition at the given experimental conditions (92). Fan et al. (92–95) demonstrated that an Fe_2O_3-based oxygen carrier can generate syngas at a concentration higher than 90%, balanced by CO_2 and steam, with full fuel conversion. In their unique moving bed reactor configuration, the reactor is designed to operate with minimal carbon deposition and without the use of steam. The feedstock can be methane, biomass, coal, and other types of carbonaceous fuels, and the H_2/CO may vary from 1:1 to 3:1 depending on the feedstock and operating conditions. Compared with NiO, iron oxides require a higher operating temperature for achieving complete methane conversion (>99%).

Other metal oxides. In addition to the three most widely studied metal oxides, CeO_2, NiO, and Fe_2O_3, several other metal oxides have been proposed as oxygen carriers for CLPO, including WO_3 and ZnO. Kodama et al. (96) found that WO_3 could oxidize methane to CO and H_2 with high selectivity without carbon deposition or without the formation of WC phase at 1,000°C. When ZrO_2 was used as the support material for WO_3, the reactivity could be improved owing to reduced grain size and improved dispersion of tungsten oxide. They further tested WO_3/ZrO_2 in a solar furnace at temperatures of 900°C–1,000°C, and the results showed that the methane conversion was higher than 80% and the CO selectivity was higher than 76% (97). The CH_4 oxidation by ZnO also generated syngas with a 2:1 H_2-to-CO ratio, and it was found that the ZnO conversion could be 90% at 1,327°C in a 5-kW prototype solar furnace. The reaction was found to be very fast. However, Zn existed in a gaseous state at high temperatures, and thus a fast quenching step was required (98). Similar studies have been carried out on MgO, SiO_2, and TiO_2; however, presently, none of them have practical use (99–101). Complex metal oxides made up of different single metal oxides were attempted to achieve more favorable performance than the performances demonstrated in single metal oxides. These results are discussed below.

Complex Metal Oxide Materials

Perovskite. Perovskite materials have been widely studied for many different applications and have also been considered as promising oxygen carrier materials for methane partial oxidation to syngas. Wei et al. (102) investigated the performance of $La_{1-x}Sr_xMO_3$ (M = Mn, Ni; x = 0–0.4) and $La_{1-x}Sr_xMnO_{3-\alpha}$, synthesized by the autocombustion method, as oxygen carrier materials.

They were able to obtain 75% CO selectivity at 16% CH_4 conversion with a H_2/CO molar ratio at 2.5:1 at 800°C. Furthermore, they investigated the effect of partial substitution of La by Sr, which resulted in an increase in reactivity and a decrease in selectivity. Dai et al. (103) synthesized $AFeO_3$ (A = La, Nd, Eu) via the sol-gel method and found that there were two stages of reactions for methane partial oxidation. In the first stage, there was a significant amount of CO_2 formation, and in the second stage, the reactions had a high selectivity toward syngas. Among these three perovskite materials, $LaFeO_3$ showed the highest selectivity. The conversion of methane and selectivity toward syngas increased with temperature. At 900°C, the methane conversion could be as high as 65% with more than 90% selectivity toward syngas if using $LaFeO_3$ as an oxygen carrier (103). These findings encouraged further studies of $LaFeO_3$ as the base structure for methane conversion. Various methods for $LaFeO_3$ synthesis have been investigated, mainly by using different complex agents, including citric acid and glycine (104). Mihai et al. (50) proposed multiple synthesis methods and found that $LaFeO_3$ prepared by a DL–tartaric acid–aided method possessed a large surface area and good reactivity. With the addition of a small amount of Sr, $La_{0.9}Sr_{0.1}FeO_3$ was found to produce even higher reactivity. They reasoned this improvement was due to increased oxygen vacancies induced by heteroatoms. Furthermore, many other types of additives have been incorporated to increase the reactivity. For example, Nalbandian et al. (105) found that $La_{0.7}Sr_{0.3}Cr_{0.05}Fe_{0.95}O_3$ mixed with 5% NiO gave excellent performance for methane partial oxidation.

$M_XFn_{3-X}O4$(M = Ni, Co, Zn, Cu, 0 < X < 1.5). Fe_3O_4 has attractive reaction properties but also has a low selectivity toward CO. To improve performance of the oxygen carrier, a series of ferrites have been synthesized from Fe_3O_4 and various types of metal oxides. For methane partial oxidation, Kodama et al. (106) investigated oxygen carriers made up of three ferrites: $Ni_{0.39}Fe_{2.61}O_4$, $Co_{0.39}Fe_{2.61}O_4$, and $Zn_{0.39}Fe_{2.61}O_4$. Under the same experimental conditions, $Co_{0.39}Fe_{2.61}O_4$ and $Zn_{0.39}Fe_{2.61}O_4$ showed poorer performance as compared with the performance of Fe_3O_4, but $Ni_{0.39}Fe_{2.61}O_4$ demonstrated a significant improvement in performance, with CO yields of 22.0% and CO selectivity of 72.2% at 827°C. The sintering properties of the oxygen carriers were also studied for ZrO_2 as a support for $Ni_{0.39}Fe_{2.61}O_4$ at a 2:1 weight ratio (106). However, low methane conversion and high carbon deposition were observed under this ZrO_2-supported condition (107). Because Ni was also widely used as a catalyst for SMR, Sturzenegger et al. (108) studied Ni-ferrite as both an oxygen carrier and a SMR catalyst. At the early stage of reduction, Ni-ferrite performed as an oxygen carrier, and at the late stage, Ni in the reduced phase acted as a SMR catalyst. An excess steam was used so that there was minimal CO in the gaseous product owing to the water-gas shift reaction. Cha et al. (109) studied $Cu_xFe_{3-x}O_4/ZrO_2$ as oxygen carriers, with x varying from 0 to 1.5 for syngas generation. Adding Cu to Fe_3O_4 decreased CH_4 conversion and selectivity. However, carbon deposition was eliminated when $0.3 < x < 0.7$. Their results indicated Cu was effective in enhancing the gasification reaction rate of deposited carbon and thus was beneficial to preventing coke formation or carbon deposition at the cost of decreasing methane conversion and CO selectivity (109). In addition, by substituting a portion of the Zr with Ce, the reaction rate for the syngas generation could be enhanced. Of the compositions studied, $Cu_{0.7}Fe_{2.3}O_4$/Ce-ZrO_2 (Ce/Zr) was found to have the best performance, with no deactivation observed within 10 cycles (110).

The materials discussed above represent the majority of oxygen carrier formulas studied. Another composition that has been investigated is NiO-Cr_2O_3-MgO. This composition showed promising behavior for methane partial oxidation for several redox cycles without significant carbon deposition. The relatively low reaction temperature, i.e., 700°C, was also an advantage. Further, adding Cr_2O_3 assisted in preventing the formation of $NiMgO_2$ and also reduced the reaction temperatures (111). To summarize, oxygen carrier materials to be employed with

industrial applications are likely to be composite metal oxides because these composite materials have shown favorable reaction behavior and can overcome some of the drawbacks of single metal oxides. However, significant research is still needed to develop a robust oxygen carrier that can provide a high fuel conversion and concurrently a high selectivity toward syngas.

PRINCIPLES FOR OXYGEN CARRIER SELECTION

The oxygen carrier designed for the chemical looping system is expected to undergo multiple redox reaction cycles with minimal loss in physical integrity and chemical reactivity. In the reduction step, the oxygen carrier donates a suitable amount of lattice oxygen for fuel conversion and product production. In the oxidation step, the depleted oxygen carriers are replenished with air while heat is released for autothermal operation. Such cyclic behavior requirement calls for certain properties to be implanted into the oxygen carrier. Extensive research has been conducted on the oxygen carrier material screening for chemical looping systems with a focus on individual aspects, such as oxygen-carrying capacity, fuel conversion, reactivity, recyclability, mechanical strength, heat-carrying capacity, melting point, and resistance to carbon deposition and contaminants. However, the applications for full oxidation and partial oxidation require some distinct oxygen carrier properties so that the product selectivity can be properly controlled. The following section discusses the thermodynamic principle for selecting active metal oxides toward various applications.

The Ellingham diagram has been widely used in metallurgic studies as a useful tool to determine the relative metal oxide reduction potential at different temperatures, as shown in **Figure 8** (112). This diagram can be further adapted for discerning metal oxides as oxygen carrier materials for various chemical looping processes (92, 93). As illustrated in **Figure 9**, materials are sorted into several zones according to their oxidation capability and their potential use as oxygen carriers for CLFO and CLPO. It should be noted that because most chemical looping processes are operated at temperatures higher than 750°C, the thermodynamic properties for metal oxides at low temperatures are not discussed here. These materials zones are outlined by the following three key reactions:

Reaction line 1: $2CO + O_2 = 2CO_2$

Reaction line 2: $2H_2 + O_2 = 2H_2O$

Reaction line 3: $2C + O_2 = 2CO$

Zone A: Metal oxides in this region stay above reaction lines 1 and 2. They generally have strong oxidizing properties and can work as oxygen carriers for both CLFO and CLPO. Metal oxides in this region include NiO, CuO, CoO, Fe_2O_3, and Fe_3O_4, as discussed in the section of Oxygen Carriers for Chemical Looping Full Oxidation.

Zone B: Metal oxides in this region stay above reaction line 3 and below reaction lines 1 and 2. They are able to work as oxygen carriers for CLPO but not for CLFO owing to their moderate oxidizing properties. Metal oxides in this region include CeO_2, as discussed in the section on Oxygen Carriers for Chemical Looping Partial Oxidation.

Zone C: Metal oxides in this region stay below reaction line 3. They cannot be used as oxygen carriers and are considered as inert materials. Metal oxides in this region include Cr_2O_3 and SiO_2.

Transition Zone: Metal oxides in this zone stay between reaction lines 1 and 2. They are considered as possible CLPO materials with a significant amount of H_2O generated in the syngas product. Metal oxides in this region include SnO_2.

From **Figure 9**, it is noted that methane is not thermodynamically stable at temperatures higher than 750°C, where methane decomposition to C and H_2 is a spontaneous reaction. Thus, the reaction line of $2CH_4 + O_2 = 2CO + 4H_2$ does not play an important role in determining zones of oxygen carriers. Metal oxides in Zone C have low oxidation capability and thus cannot

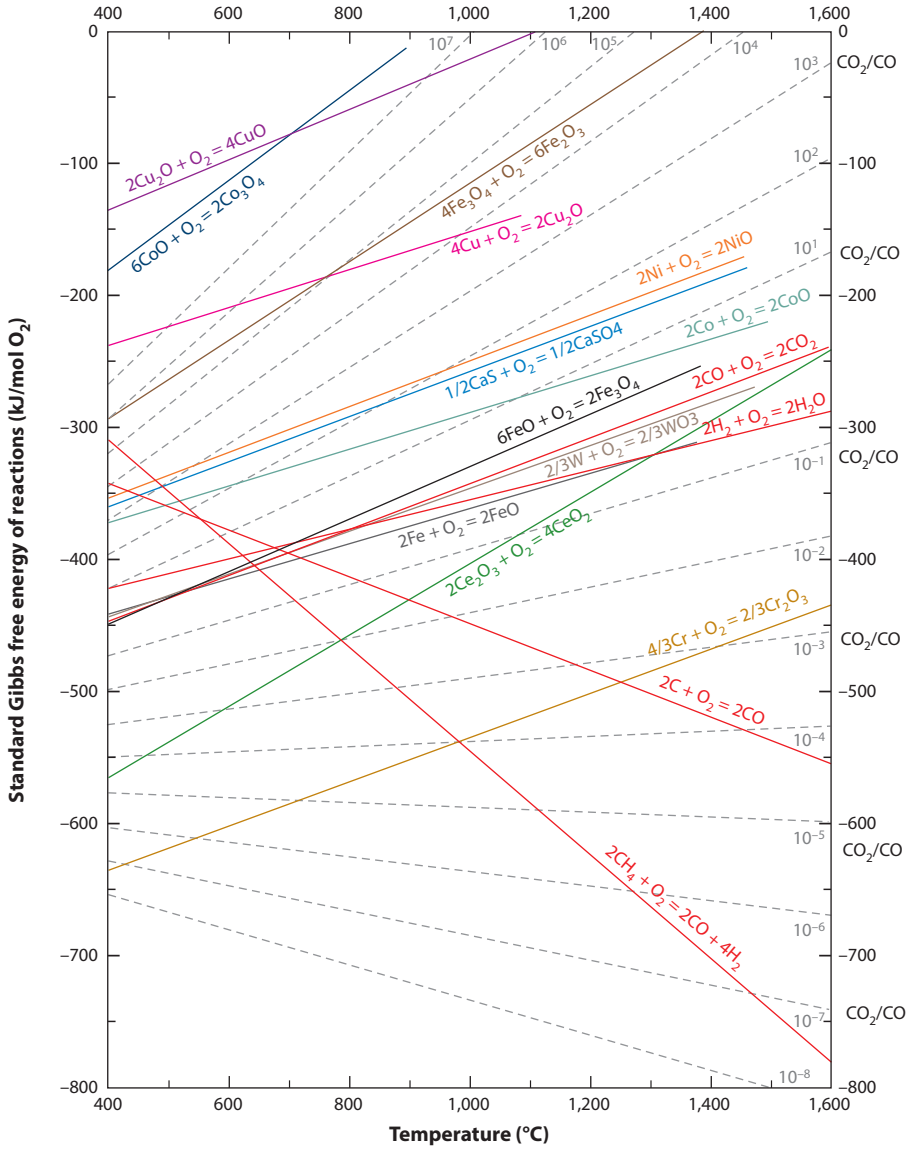

Figure 8

Ellingham diagram for oxygen carrier comparison (111).

be directly used for chemical looping applications. However, they can be used as inert support materials or active components together with materials in Zones A and B, forming composite oxygen carriers. The interaction among these metal oxides can have a negative or positive effect on the performance of the oxygen carrier. For example, CuO in Zone A and Al_2O_3 in Zone C would form $CuAl_2O_4$, resulting in a loss of copper oxide's unique CLOU property (23). FeO in Zone B and TiO_2 in Zone C could form $FeTiO_3$, prompting oxygen ion diffusion and thus increasing the oxygen carrier reactivity (67). This highlights the importance of knowing the various solid phases present in the oxygen carrier, as it can alter the performance of the oxygen carrier.

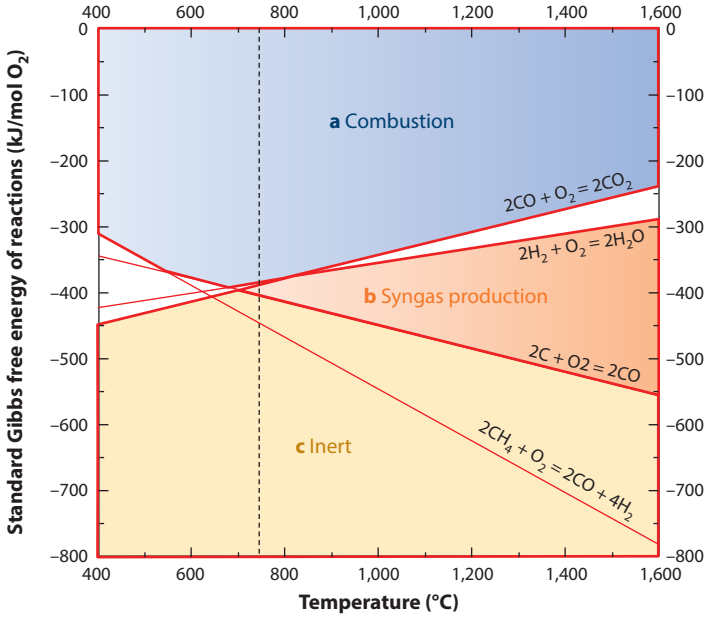

Figure 9

Zone of metal oxides for chemical looping.

For CLFO or combustion applications, the primary metal oxides should be selected from Zone A. The major merit of the CLFO systems is the ability to achieve in situ CO_2 capture with reduced cost. CO_2 purity associated with the oxygen carrier is an important property because of its direct impact on the energy conversion efficiencies and the commercial viability of the CLFO system. The selection of the active metal oxide influences the maximum fuel conversion and CO_2 purity achievable based on thermodynamic constraints. To elaborate, from the reaction thermodynamics, using iron- or copper-based oxygen carriers can result in 100% fuel conversion to CO_2 and H_2O, whereas using nickel oxide– or calcium sulfate–based oxygen carriers can yield at most 99% fuel conversion with considerable amounts of CO leakage. For solid fuel conversion, metal oxides with CLOU features are preferred, as they can release gaseous oxygen for carbon gasification. However, the stability of CLOU materials must be further improved.

There are typically two approaches to reach the targeted syngas products in the CLPO processes. The first approach is to use oxygen carriers in Zone A. For oxygen carriers in Zone A, which are applicable to both partial oxidation and combustion, the amount of oxygen transferred from the oxygen carrier to the fuel species determines whether the product is syngas or CO_2 and H_2O. Partial oxidation of fuel requires less oxygen transferred from the metal oxides than in full combustion for a given feedstock. For metal oxides in Zone A, such as NiO, the syngas yield increases initially until the stoichiometric ratio for methane partial oxidation is exceeded. The syngas yield decreases afterward owing to the oxidation of syngas to CO_2 and H_2O. The conduct of CLPO in existing fluidized bed reactors usually adopts this approach. As an example, in CSIC's circulating fluidized bed–based CLR process, the air consumed in the combustor was adjusted to produce a mixture of NiO and Ni at approximately 70% Ni and 30% NiO rather than 100% NiO. The partially regenerated oxygen carriers were then reduced by methane in the reducer to a composition of 80% Ni and 20% NiO (87). The circulation rate for the oxygen carrier materials in this approach would be substantial because of the low oxygen-carrier capacity.

In addition to the low oxygen-carrier conversion, excess steam was introduced into the reducer to suppress the carbon deposition because metallic nickel also served as an effective catalyst for the methane decomposition reaction. Further, the syngas composition varies significantly with nickel oxide conversion and thus is difficult to control using materials in Zone A. The second approach is to adopt metal oxides in Zone B. The syngas composition is dominated by H_2 and CO with oxygen carriers in Zone B owing to their thermodynamic restriction. For metal oxides in Zone B, such as CeO_2, syngas yield increases linearly, reaching the maximum at the stoichiometric ratio for partial oxidation, and remains constant. For metal oxides that have multiple oxidation states, such as iron oxides, the syngas yield line shows an integrated pattern of individual syngas lines of Fe_2O_3 (Zone A), Fe_3O_4 (Zone A), and FeO (Zone B). Reactions conducted in the moving bed reactor are suggested to employ this approach to better control the metal oxide reduction extent and syngas composition (92). In a moving bed reactor, the synergistic effects of the fuel and the oxygen carrier in Zone B may yield a steady syngas product while the oxygen carrier oxidation state varies. Further, such a scheme could assist in inhibiting methane decomposition by using a certain range of oxygen carrier composition, even without the need of external steam. It is noted that the adapted Ellingham diagram provides only a thermodynamic indication of the possibility of metal oxides acting as oxygen carriers. The reaction kinetics, reactant stoichiometry, gas-solid flow dynamics, contact time, and reactor design altogether determine the actual reaction performance.

SUMMARY

Recent advances in oxygen carrier materials development for CLFO and CLPO processes are discussed in this review. Based on the thermodynamic properties, oxygen carriers for CLFO can be grouped into metal oxides with CLOU features and metal oxides without CLOU features. Generally, the former group exhibits a higher rate of reactions, whereas the latter group exhibits a higher stability in cyclic reactor operation. Metal oxides have also been investigated for CLPO application under different operation conditions. Most of the oxygen carriers being considered for CLC and CLG are single metal oxides, e.g., NiO and Fe_2O_3, supported by inert materials, e.g., $MgAl_2O_4$, Al_2O_3, TiO_2, and SiO_2. Complex metal oxides, such as materials with perovskite structures, are considered at the lab-scale operation, where they are synthesized and tested with superior performance as compared with the performance of single metal oxide materials. However, considerable opportunity for improvement exists for these materials, particularly with respect to durability, cost of materials, and synthesis techniques for sustainable performance. A general approach for predicting the feasibility of metal oxides as oxygen carriers for CLFO and CLPO process applications is illustrated in light of an adapted Ellingham diagram.

In addition to the metal oxide particle properties and performances discussed above, reactor design, specifically gas and solid contact modes, is another important factor governing the success of chemical looping systems. The reactor design requires comprehensive understanding of the thermodynamic properties of the oxygen carrier materials, their reaction kinetics, and the flow dynamics of fluid and particles in the reactor. Further, the oxygen carrier development and reactor design should also be considered from the overall process system point of view. It is anticipated that with appropriate oxygen carrier development coupled with desired reactor configurations, chemical looping systems can be efficiently applied for generation of a variety of products from gaseous, liquid, or solid carbonaceous feedstock.

DISCLOSURE STATEMENT

The authors are not aware of any affiliations, memberships, funding, or financial holdings that might be perceived as affecting the objectivity of this review.

ACKNOWLEDGMENTS

The authors would like to thank Dr. Lang Qin, Mr. Dikai Xu, Dr. Andrew Tong, and Mr. Cheng Chung for their helpful discussion during the preparation of this manuscript.

LITERATURE CITED

1. US Energy Inf. Adm. 2013. *International Energy Outlook 2013*. Washington, DC: US Energy Inf. Adm.
2. US Natl. Ocean. Atmos. Adm. 2013. *Trends in Atmospheric Carbon Dioxide 2013*. Mauna Loa, HI: US Natl. Ocean. Atmos. Adm.
3. Figueroa JD, Fout T, Plasynski S, McIlvried H, Srivastava RD. 2008. Advances in CO_2 capture technology—the U.S. Department of Energy's carbon sequestration program. *Int. J. Greenh. Gas Control* 2:9–20
4. Fan LS. 2010. *Chemical Looping Systems for Fossil Energy Conversions*. New York: Wiley
5. Fan LS, Zeng L, Wang W, Luo S. 2012. Chemical looping processes for CO_2 capture and carbonaceous fuel conversion—prospect and opportunity. *Energy Environ. Sci.* 5:7254–80
6. Connell DP, Dunkerley ML, Lewandowski DA, Zeng L, Wang D, et al. 2012. Techno-economic analysis of a coal direct chemical looping power plant with carbon dioxide capture. *Int. Tech. Conf. Clean Coal Fuel Syst.* 37:11–22
7. Xu J, Froment GF. 1989. Methane steam reforming, methanation and water-gas shift: I. Intrinsic kinetics. *AIChE J.* 35:88–96
8. Tang P, Zhu Q, Wu Z, Ma D. 2014. Methane activation: the past and future. *Energy Environ. Sci.* 7:2580–91
9. Shafiefarhood A, Galinsky N, Huang Y, Chen Y, Li F. 2014. Fe_2O_3@$La_xSr_{1-x}FeO_3$ core-shell redox catalyst for chemical looping reforming of methane. *ChemCatChem* 6(3):790–99
10. He F, Trainham J, Parsons G, Newman JS, Li F. 2014. A hybrid solar-redox scheme for liquid fuel and hydrogen coproduction. *Energy Environ. Sci.* 7:2033–42
11. Thursfield A, Murugan A, Franca R, Metcalfe IS. 2012. Chemical looping and oxygen permeable ceramic membranes for hydrogen production—a review. *Energy Environ. Sci.* 5:7421–59
12. Adánez J, de Diego LF, García-Labiano F, Gayán P, Abad A. 2004. Selection of oxygen carriers for chemical-looping combustion. *Energy Fuels* 18:371–77
13. Li F, Kim H, Sridhar D, Wang F, Zeng L, et al. 2009. Syngas chemical looping gasification process: oxygen carrier particle selection and performance. *Energy Fuels* 23:4182–89
14. Mattisson T, Leion H, Lyngfelt A. 2009. Chemical-looping with oxygen uncoupling using CuO/ZrO_2 with petroleum coke. *Fuel* 88:683–90
15. Lewis WK, Gilliland ER, Sweeney WP. 1951. Gasification of carbon metal oxides in a fluidized powder bed. *Chem. Eng. Prog.* 47(5):251–56
16. Zhu Y, Mimura K, Isshiki M. 2004. Oxidation mechanism of Cu_2O to CuO at 600–1050°C. *Oxid. Met.* 62:207–22
17. de Diego LF, García-Labiano F, Adánez J, Gayán P, Abad A, et al. 2004. Development of Cu-based oxygen carriers for chemical-looping combustion. *Fuel* 83(13):1749–57
18. de Diego LF, Gayán P, García-Labiano F, Celaya J, Abad A, et al. 2005. Impregnated CuO/Al_2O_3 oxygen carriers for chemical-looping combustion: avoiding fluidized bed agglomeration. *Energy Fuels* 19(5):1850–56
19. Gayán P, Forero CR, Abad A, de Diego LF, García-Labiano F, et al. 2007. Effect of support on the behavior of Cu-based oxygen carriers during long-term CLC operation at temperatures above 1073 K. *Energy Fuels* 25(3):1316–26
20. Forero CR, Gayán P, García-Labiano F, de Diego LF, Abad A, et al. 2010. Effect of gas composition in chemical-looping combustion with copper-based oxygen carriers: fate of sulphur. *Int. J. Greenh. Gas Control* 4:762–70
21. Adánez-Rubio I, Gayán P, García-Labiano F, de Diego LF, Adánez J, et al. 2011. Development of CuO-based oxygen-carrier materials suitable for chemical-looping with oxygen uncoupling (CLOU) process. *Energy Procedia* 4:417–24

22. Gayán P, Adánez-Rubio I, Abad A, de Diego LF, García-Labiano F, et al. 2012. Development of Cu-based oxygen carriers for chemical-looping with oxygen uncoupling (CLOU) process. *Fuel* 96:226–38
23. Arjmand M, Azad AM, Leion H, Lyngfelt A, Mattisson T. 2011. Prospects of Al_2O_3 and $MgAl_2O_4$-supported CuO oxygen carriers in chemical-looping combustion (CLC) and chemical-looping with oxygen uncoupling (CLOU). *Energy Fuels* 25:5493–502
24. Arjmand M, Keller M, Leion H, Mattisson T, Lyngfelt A. 2012. Oxygen release and oxidation rates of $MgAl_2O_4$ supported CuO oxygen carrier for chemical-looping combustion with oxygen uncoupling (CLOU). *Energy Fuels* 26:6528–39
25. Xu L, Wang J, Li Z, Cai N. 2013. Experimental study of cement-supported CuO oxygen carriers in chemical looping with oxygen uncoupling (CLOU). *Energy Fuels* 27:1522–30
26. Song Q, Liu W, Bohn CD, Harper RN, Sivaniah E, et al. 2013. A high performance oxygen storage material for chemical looping processes with CO_2 capture. *Energy Environ. Sci.* 6:288–98
27. Thomas TJ, Fan LS, Gupta P, Valazquez-Vargas LG. 2010. *Combustion looping using composite oxygen carriers.* US Patent No. 7767191
28. Li F, Zeng L, Velazquez-Vargas LG, Yoscovits Z, Fan L-S. 2010. Syngas chemical looping gasification process: bench scale studies and reactor simulations. *AIChE J.* 56:2186–99
29. Sridhar D, Tong A, Kim HR, Zeng L, Li F, et al. 2012. Syngas chemical looping process: design and construction of a 25 kW_{th} subpilot unit. *Energy Fuels* 26(4):2292–302
30. Tong A, Sridhar D, Sun Z, Kim HR, Zeng L, et al. 2013. Continuous high purity hydrogen generation from a syngas chemical looping 25 kW_{th} subpilot unit with 100% carbon capture. *Fuel* 103:495–595
31. Kim HR, Wang D, Zeng L, Bayham S, Tong A, et al. 2013. Coal direct chemical looping combustion process: design and operation of a 25-kW_{th} sub-pilot unit. *Fuel* 108:370–84
32. Tong A, Zeng L, Kathe M, Sridhar D, Fan L-S. 2013. Application of the moving bed chemical looping process for high methane conversion. *Energy Fuels* 27:4119–28
33. Bayham S, Kim HR, Wang D, Tong A, Zeng L, et al. 2013. Iron-based coal direct chemical looping combustion process: 200-hour continuous operation of a 25 kW_{th} sub-pilot unit. *Energy Fuels* 27(3):1347–56
34. Pineau A, Kanari N, Gaballah I. 2006. Kinetics of reduction of iron oxides by H_2 part I: low temperature reduction of hematite. *Thermochim. Acta* 447:89–100
35. Pineau A, Kanari N, Gaballah I. 2007. Kinetics of reduction of iron oxides by H_2 part II: low temperature reduction of magnetite. *Thermochim. Acta* 456:75–88
36. Li S, Krishnamoorthy S, Li A, Meitzner GD, Iglesia E. 2002. Promoted iron-based catalysts for the Fischer–Tropsch synthesis: design, synthesis, site densities, and catalytic properties. *J. Catal.* 206:202–17
37. Chen S, Shi Q, Xue Z, Sun X, Xiang W. 2011. Experimental investigation of chemical-looping hydrogen generation using Al_2O_3 or TiO_2-supported iron oxides in a batch fluidized bed. *Int. J. Hydrog. Energy* 36:8915–26
38. Liu L, Zachariah MR. 2013. Enhanced performance of alkali metal doped Fe_2O_3 and Fe_2O_3/Al_2O_3 composites as oxygen carrier material in chemical looping combustion. *Energy Fuels* 27:4977–83
39. Li F, Sun Z, Luo S, Fan LS. 2011. Ionic diffusion in the oxidation of iron-effect of support and its implications to chemical looping applications. *Energy Environ. Sci.* 4:876–80
40. Song Q, Xiao R, Deng Z, Zheng W, Shen L, et al. 2008. Multicycle study on chemical-looping combustion of simulated coal gas with a $CaSO_4$ oxygen carrier in a fluidized bed reactor. *Energy Fuels* 22:3661–72
41. Song T, Zheng M, Shen L, Zhang T, Niu X, et al. 2013. Mechanism investigation of enhancing reaction performance with $CaSO_4/Fe_2O_3$ oxygen carrier in chemical-looping combustion of coal. *Ind. Eng. Chem. Res.* 52:4059–71
42. He F, Galinsky N, Li F. 2013. Chemical looping gasification of solid fuels using bimetallic oxygen carrier particles—feasibility assessment and process simulations. *Int. J. Hydrog. Energy* 38:7839–54
43. Shulman A, Cleverstam E, Mattisson T, Lyngfelt A. 2009. Manganese/iron, manganese/nickel, and manganese/silicon oxides used in chemical-looping with oxygen uncoupling (CLOU) for combustion of methane. *Energy Fuels* 23:5269–75
44. Azimi G, Ryden M, Leion H, Mattisson T, Lyngfelt T. 2012. $(Mn_zFe_{1-z})_yO_x$ combined oxides as oxygen carrier for chemical-looping with oxygen uncoupling. *AIChE J.* 59:582–88

45. Azimi G, Leion H, Ryden M, Mattisson T, Lyngfelt T. 2013. Investigation of different Mn–Fe oxides as oxygen carrier for chemical-looping with oxygen uncoupling (CLOU). *Energy Fuels* 27:367–77
46. Azad A, Hedayati A, Ryden M, Leion H, Mattisson T. 2013. Examining the Cu–Mn–O spinel system as an oxygen carrier in chemical looping combustion. *Energy Technol.* 1:59–69
47. Shen S, Li R, Zhou J, Yu C. 2003. Selective oxidation of light hydrocarbons using lattice oxygen instead of molecular oxygen. *Chin. J. Chem. Eng.* 11:649–54
48. Dai X, Wu Q, Li R, Yu C, Hao Z. 2006. Hydrogen production from a combination of the water–gas shift and redox cycle process of methane partial oxidation via lattice oxygen over $LaFeO_3$ perovskite catalyst. *J. Phys. Chem. B* 110:25856–62
49. Galinsky NL, Huang Y, Shafiefarhood A, Li F. 2013. Iron oxide with facilitated O_2– transport for facile fuel oxidation and CO_2 capture in a chemical looping scheme. *ACS Sustain. Chem. Eng.* 1:364–73
50. Mihai O, Chen D, Holmen A. 2011. Catalytic consequence of oxygen of lanthanum ferrite Perovskite in chemical looping reforming of methane. *Ind. Eng. Chem. Res.* 50:2613–21
51. Carter S, Selcuk A, Chater R, Kajda J, Kilner J, et al. 1992. Oxygen transport in selected nonstoichiometric perovskite-structure oxides. *Solid State Ionics* 53:597–605
52. Bakken E, Norby T, Stølen S. 2005. Nonstoichiometry and reductive decomposition of $CaMnO_3$. *Solid State Ionics* 176:217–23
53. Leion H, Larring Y, Bakken E, Bredesen R, Mattisson T, et al. 2009. Use of CaMn0.875Ti0.125O3 as oxygen carrier in chemical-looping with oxygen uncoupling. *Energy Fuels* 23:5276–83
54. Hallberg P, Jing D, Ryden M, Mattisson T, Lynfelt A. 2013. Chemical looping combustion and chemical looping with oxygen uncoupling experiments in a batch reactor using spray-dried $CaMn_{1-x}M_xO_{3-\delta}$ (M = Ti, Fe, Mg) particles as oxygen carriers. *Energy Fuels* 27:1473–81
55. Arjmand M, Hedayati A, Azad AM, Leion H, Ryden M, et al. 2013. $Ca_xLa_{1-x}Mn_{1-y}M_yO_{3-\delta}$ (M = Mg, Ti, Fe, or Cu) as oxygen carriers for chemical-looping with oxygen uncoupling (CLOU). *Energy Fuels* 27:4097–107
56. Sundqvist S, Leion H, Ryden M, Lyngfelt A, Mattisson T. 2013. CaMn0.875Ti0.125O3−δ as an oxygen carrier for chemical-looping with oxygen uncoupling (CLOU)—solid-fuel testing and sulfur interaction. *Energy Technol.* 1:338–44
57. Peña JA, Lorente E, Romero E, Herguido J. 2006. Kinetic study of the redox process for storing hydrogen reduction stage. *Catal. Today* 116:439–44
58. Kuo YL, Hsu WM, Chiu PC, Tseng YH, Ku Y. 2013. Assessment of redox behavior of nickel ferrite as oxygen carriers for chemical looping process. *Ceram. Int.* 39:5459–65
59. Wang B, Yan R, Zhao H, Zheng Y, Liu Z, Zheng C. 2011. Investigation of chemical looping combustion of coal with $CuFe_2O_4$ oxygen carrier. *Energy Fuels* 25:3344–54
60. Wang B, Zhao H, Zheng Y, Liu Z, Zheng C. 2013. Chemical looping combustion of petroleum coke with $CuFe_2O_4$ as oxygen carrier. *Chem. Eng. Technol.* 36:1488–95
61. Scheffe JR, Allendorf MD, Coker EN, Jacobs BW, McDaniel AH, et al. 2011. Hydrogen production via chemical looping redox cycles using atomic layer deposition-synthesized iron oxide and cobalt ferrites. *Chem. Mater.* 23:2030–38
62. Muhich CL, Evanko BW, Weston KC, Lichty P, Liang X, et al. 2013. Efficient generation of H_2 by splitting water with an isothermal redox cycle. *Science* 341:540–42
63. Leion H, Lyngfelt A, Johansson M, Jerndal E, Mattisson T. 2008. The use of ilmenite as an oxygen carrier in chemical-looping combustion. *Chem. Eng. Res. Des.* 86:1017–26
64. Gu H, Shen L, Xiao J, Zhang S, Song T. 2011. Chemical looping combustion of biomass/coal with natural iron ore as oxygen carrier in a continuous reactor. *Energy Fuels* 25:446–55
65. Cuadrat A, Abad A, Adánez J, de Diego LF, García-Labiano F, Gayán P. 2012. Behavior of ilmenite as oxygen carrier in chemical-looping combustion. *Fuel Process. Technol.* 94:101–12
66. Tian H, Siriwardane R, Simonyi T, Poston J. 2013. Natural ores as oxygen carriers in chemical looping combustion. *Energy Fuels* 27:4108–18
67. Li F, Luo S, Sun Z, Bao X, Fan LS. 2011. Role of metal oxide support in redox reactions of iron oxide for chemical looping applications: experiments and density functional theory calculations. *Energy Envir. Sci.* 4:3661–67

68. Li K, Wang H, Wei Y. 2013. Syngas generation from methane using a chemical looping concept: a review of oxygen carriers. *J. Chem.* 2013:294817
69. Otsuka K, Wang Y, Sunada E, Yamanaka I. 1998. Direct partial oxidation of methane to synthesis gas by cerium oxide. *J. Catal.* 175:152–60
70. Gupta A, Hegde MS, Priolkar KR, Waghmare UV, Sarode PR, et al. 2009. Structural investigation of activated lattice oxygen in $Ce_{1-x}Sn_xO_2$ and $Ce_{1-x-y}Sn_xPd_yO_{2-\delta}$ by EXAFS and DFT calculation. *Chem. Mater.* 21:5836–47
71. Wang S, Kobayashi T, Dokiya M, Hashimoto T. 2000. Electrical and ionic conductivity of Gd-doped ceria. *J. Electrochem. Soc.* 147:3606–9
72. Salazar-Villalpando MD, Berry DA, Cugini A. 2010. Role of lattice oxygen in the partial oxidation of methane over Rh/zirconia-doped ceria. Isotopic studies. *Int. J. Hydrog. Energy* 36:1998–2003
73. Mattos LV, Rodino E, Resasco DE, Passos FB, Noronha FB. 2003. Partial oxidation and CO_2 reforming of methane on Pt/AL_2O_3, Pt/ZrO_2 and $Pt/Ce\text{-}ZrO_2$ catalysts. *Fuel Process. Technol.* 83:147–61
74. Wu Q, Chen J, Zhang J. 2008. Effect of yttrium and praseodymium on properties of $Ce_{0.75}Zr_{0.25}O_2$ solid solution for CH_4–CO_2 reforming. *Fuel Process. Technol.* 89:993–99
75. Sadykov VA, Kuznetsova TG, Alikina GM, Frolova YV, Lukashevich AI, et al. 2004. Ceria-based fluorite-like oxide solid solutions as catalysts of methane selective oxidation into syngas by the lattice oxygen: synthesis, characterization and performance. *Catal. Today* 93:45–53
76. Kang ZC, Eyring L. 2000. Lattice oxygen transfer in fluorite-type oxides containing Ce, Pr, and/or Tb. *J. Solid State Chem.* 155:129–37
77. Jalibert JC, Fathi M, Rokstad OA, Holmen A. 2001. Synthesis gas production by partial oxidation of methane from the cyclic gas-solid reaction using promoted cerium oxide. *Stud. Surf. Sci. Catal.* 136:301–6
78. Li R, Yu C, Dai X, Shen S. 2002. Partial oxidation of methane to synthesis gas using lattice oxygen instead of molecular oxygen. *Chin. J. Catal.* 10:56–69
79. Jeong HH, Kwak JH, Han GY, Yoon KJ. 2011. Stepwise production of syngas and hydrogen through methane reforming and water splitting by using a cerium oxide redox system. *Int. J. Hydrog. Energy* 36:15221–30
80. Chen J, Yao C, Zhao Y, Jia P. 2010. Synthesis gas production from dry reforming of methane over $Ce_{0.75}Zr_{0.25}O_2$-supported Ru catalysts. *Int. J. Hydrog. Energy* 35:1630–42
81. Johansson M, Mattisson T, Lyngfelt A, Abad A. 2008. Using continuous and pulse experiments to compare two promising nickel-based oxygen carriers for use in chemical-looping technologies. *Fuel* 87:988–1001
82. de Diego LF, Ortiz M, Adánez J, García-Labiano F, Abad A, Gayán P. 2008. Synthesis gas generation by chemical-looping reforming in a batch fluidized bed reactor using Ni-based oxygen carriers. *Chem. Eng. J.* 144:289–98
83. Jerndal E, Mattisson T, Lyngfelt A. 2009. Investigation of $NiO/NiAl_2O_4$ oxygen carriers for chemical-looping combustion produced by spray-drying. *Energy Fuels* 23:665–76
84. Zafar Q, Mattisson T, Gevert B. 2006. Redox investigation of some oxides of transition-state metals Ni, Cu, Fe, and Mn supported on SiO_2 and $MgAl_2O_4$. *Energy Fuels* 20:34–44
85. Adánez J, Abad A, García-Labiano F, Gayán P, de Diego LF. 2012. Progress in chemical-looping combustion and reforming technologies. *Prog. Energy Combust.* 38:215–82
86. Ryden M, Lyngfelt A, Mattisson T. 2006. Synthesis gas generation by chemical-looping reforming in a continuously operating laboratory reactor. *Fuel* 85:1631–41
87. de Diego LF, Ortiz M, García-Labiano F, Adánez J, Abad A, et al. 2009. Hydrogen production by chemical-looping reforming in a circulating fluidized bed reactor using Ni-based oxygen carriers. *J. Power Sources* 192:27–34
88. Pröll T, Bolhàr-Nordenkampf J, Kolbitsch P, Hofbauer H. 2010. Syngas and a separate nitrogen/argon stream via chemical looping reforming—a 140 kW pilot plant study. *Fuel* 89:1249–56
89. Azadi P, Otomo J, Hatano H, Oshima Y, Farnood R. 2011. Interactions of supported nickel and nickel oxide catalysts with methane and steam at high temperatures. *Chem. Eng. Sci.* 66:4196–202
90. Nakayama O, Ikenaga N, Miyake T, Yagasaki E, Suzuki T. 2008. Partial oxidation of CH_4 with air to produce pure hydrogen and syngas. *Catal. Today* 138:141–46

91. Steinfeld A, Kuhn P. 1993. High-temperature solar thermochemistry: production of iron and synthesis gas by Fe_3O_4-reduction with methane. *Energy* 18:239–49
92. Fan LS, Luo S, Zeng L. 2013. *Methods for fuel conversion*. US Provis. Patent Appl. No. PCT/US2014/014877
93. Fan LS, Luo S, Zeng L, Xu D. 2013. *High quality syngas production using composite metal oxides*. US Provis. Patent Appl. No. 61/875,425
94. Fan LS, Wang D. 2013. *Devices and methods for co-current chemical looping system*. US Provis. Patent Appl. No. OSU0082MA
95. Fan LS, Kathe M, Wang W, Chung E, Tong A. 2014. *Novel chemical looping process configurations*. US Provis. Patent Appl. No. 61/945,257
96. Kodama T, Ohtake H, Matsumoto S, Aoki A, Shimizu T, Kitayama Y. 2000. Thermochemical methane reforming using a reactive WO_3/W redox system. *Energy* 25:411–25
97. Kodama T, Shimizu T, Satoh T, Shimizu KI. 2003. Stepwise production of CO-rich syngas and hydrogen via methane reforming by a WO_3-redox catalyst. *Energy* 28:1055–68
98. Steinfeld A, Brack M, Meier A, Weidenkaff A, Wuillemin D. 1998. A solar chemical reactor for co-production of zinc and synthesis gas. *Energy* 18:239–49
99. Kodama T, Miura S, Shimizu T, Kitayama Y. 1997. Thermochemical conversion of coal and water to CO and H_2 by a two-step redox cycle of ferrite. *Energy* 22:1019–27
100. Aoki A, Shimizu T, Kitayama Y, Kodama T. 1999. A two-step thermochemical conversion of CH_4 to CO, H_2 and C_2-hydrocarbons below 1173 K. *J. Phys. IV France* 9:337–42
101. Halmann M, Frei A, Steinfeld A. 2002. Thermo-neutral production of metals and hydrogen or methanol by the combined reduction of the oxides of zinc or iron with partial oxidation of hydrocarbons. *Energy* 27:1069–84
102. Wei HJ, Cao Y, Ji WJ, Au CT. 2008. Lattice oxygen of $La_{1-x}Sr_xMO_3$ (M = Mn, Ni) and $LaMnO_{3-a}F_b$ perovskite oxides for the partial oxidation of methane to synthesis gas. *Catal. Commun.* 9:2509–12
103. Dai X, Li R, Yu C, Hao Z. 2006. Unsteady-state direct partial oxidation of methane to synthesis gas in a fixed-bed reactor using $AFeO_3$ (A = La, Nd, Eu) perovskite-type oxides as oxygen storage. *J. Phys. Chem. B* 110:22525–31
104. Wang Y, Zhu Y, Zhang L, Yang X, Lu L, Wang X. 2006. Preparation and characterization of perovskite $LaFeO_3$ nanocrystals. *Mater. Lett.* 60:1767–70
105. Nalbandian L, Evdou A, Zaspalis V. 2011. $La_{1-x}Sr_xM_yFe_{1-y}O_{3-z}$ perovskites as oxygen-carrier materials for chemical-looping reforming. *Int. J. Hydrog. Energy* 36:6657–70
106. Kodama T, Shimizu T, Satoh T, Nakata M, Shimizu KI. 2002. Stepwise production of CO-rich syngas and hydrogen via solar methane reforming by using a Ni(II)–ferrite redox system. *Sol. Energy* 73:363–74
107. Trimm DL. 1999. Catalysts for the control of coking during steam reforming. *Catal. Today* 49:3–10
108. Sturzenegger M, D'Souza L, Struis RP, Stucki S. 2006. Oxygen transfer and catalytic properties of nickel iron oxides for steam reforming of methane. *Fuel* 85:1599–602
109. Cha KS, Yoo BK, Kim HS, Ryu TG, Kang KS, et al. 2010. A study on improving reactivity of Cu-ferrite/ZrO_2 medium for syngas and hydrogen production from two-step thermochemical methane reforming. *Energy* 34:422–30
110. Cha KS, Kim HS, Yoo BK, Lee YS, Kang KS, et al. 2009. Reaction characteristics of two-step methane reforming over a Cu-ferrite/Ce–ZrO_2 medium. *Int. J. Hydrog. Energy* 34:1801–8
111. Nakayama O, Ikenaga N, Miyake T, Yagasaki E, Suzuki T. 2010. Production of synthesis gas from methane using lattice oxygen of NiO–Cr_2O_3–MgO complex oxide. *Ind. Eng. Chem. Res.* 49:526–34
112. Paul A. 1985. Effect of thermal stabilization on redox equilibria and colour of glass. *J. Non-Cryst. Solids* 71:269–78